GEOPHYSICS, VOL. 84, NO. 1 (JANUARY-FEBRUARY 2019); P. A19–A24, 3 FIGS., 1 TABLE.
10.1190/GEO2018-0430.1

Slant *f-k* transform of multichannel seismic surface wave data

Aleksander S. Serdyukov[1], Aleksander V. Yablokov[1], Anton A. Duchkov[2], Anton A. Azarov[3], and Valery D. Baranov[4]

ABSTRACT

We have addressed the problem of estimating surface-wave phase velocities through the spectral processing of seismic data. This is the key step of the well-known near-surface seismic exploration method, called multichannel analysis of surface waves. To increase the accuracy and ensure the unambiguity of the selection of dispersion curves, we have developed a new version of the frequency-wavenumber (f-k) transform based on the S-transform. We obtain the frequency-time representation of seismic data. We analyze the obtained S-transform frequency-time representation in a slant-stacking manner but use a spatial Fourier transform instead of amplitude stacking. Finally, we build the f-k image by analyzing the spatial spectra for different steering values of the surface-wave group velocities. The time localization of the surface-wave packet at each frequency increases the signal-to-noise ratio because of an exclusion of noise in other time steps (which does not fall in the effective width of the corresponding wavelet). The new f-k transform, i.e., the slant f-k (SFK) transform, renders a better spectral analysis than the conventional f-k transform and yields more accurate phase-velocity estimation, which is critical for the surface-wave analysis. The advantages of the SFK transform have been confirmed by synthetic- and field-data processing.

INTRODUCTION

The multichannel analysis of surface waves (MASW) (Park et al., 1999; Socco et al., 2010) is a well-known method to estimate shear velocities through the inversion of the surface-wave phase-velocity dispersion curves. The MASW is widely applied to investigate soil structures for geotechnical purposes. In the field of hydrocarbon seismic exploration, surface-wave analysis can be used to compute the receiver static corrections for body-wave processing (Mari, 1984; Askari et al., 2015).

A key step of the MASW is to transform the data from the time-space (t-x) domain to the frequency-phase-velocity (f-v) domain. Common approaches to perform this transformation are slant-stack (τ-p) (McMechan and Yedlin, 1981) and frequency-wavenumber (f-k) (Yilmaz, 1987) transforms and the phase-shift method (Park et al., 1998). As shown in Shen et al. (2015), these methods yield equivalent results (at least for noise-free data). Luo et al. (2008) claim that, compared with the slant-stacking algorithm, high-resolution linear Radon transform (Sacchi and Ulrych, 1995) can improve the resolution of images of Rayleigh-wave dispersion energy. A frequency decomposition and slant stacking (Park et al., 1998; Xia et al., 2007) provides better results than that of τ-p transformation because frequencies are decomposed before slant stacking. For noisy field data, the dispersion curves are manually selected. The operator should often empirically plot a smooth and realistic dispersion curve. The images are sometimes so distorted that it is difficult to distinguish dispersion trend of the surface wave. To increase the accuracy and ensure the unambiguity of the selection of a surface-wave dispersion curve, we introduce a new f-k spectral imaging method, which is called the slant f-k (SFK) transform.

Our proposed technique is based on time-frequency analysis using the S-transform method, which was introduced by Stockwell

Manuscript received by the Editor 9 June 2018; revised manuscript received 15 August 2018; published ahead of production 12 October 2018; published online 13 December 2018.
[1]Trofimuk Institute of Petroleum Geology and Geophysics, 2 Koptuga Avenu, Novosibirsk 630090, Russia, N. A. Chinakal Institute of Mining, 54 Krasny Avenue, Novosibirsk 630091, Russia, and Novosibirsk State University, 1 Pirogova Street, Novosibirsk 630090, Russia. E-mail: aleksanderserdyukov@yandex.ru (corresponding author); yablokov.alexandr93@gmail.com.
[2]Trofimuk Institute of Petroleum Geology and Geophysics, 2 Koptuga Avenue, Novosibirsk 630090, Russia and Novosibirsk State University, 1 Pirogova Street, Novosibirsk 630090, Russia. E-mail: duchkovaa@ipgg.sbras.ru.
[3]N. A. Chinakal Institute of Mining, 54 Krasny Avenue, Novosibirsk 630091, Russia. E-mail: antonazv@mail.ru.
[4]Technologies of Inverse Problems Ltd., 3rd Kadashevsky Pereulok, 6 pp., Moscow 115035, Russia. E-mail: bvd@cntb.ru.

et al. (1996). The S-transform has been widely used in different seismic data-processing applications (Tian et al., 2002; Pinnegar and Eaton, 2003; Li et al., 2016). Inspired by the series of publications (Askari and Siahkoohi, 2008; Askari and Ferguson, 2012; Askari and Hejazi, 2015), in which the S-transform was applied to analyze the surface-wave propagation, we suggest a method to obtain f-k images with dramatically amplified surface waves. Our method expands the idea of slant stacking the S-transform spectral amplitudes, which was proposed by Askari and Hejazi (2015) to estimate the surface-wave group velocities. We use the amplitude and phase spectrum of the S-transform, which enables us to estimate the phase velocities in the f-k image analysis during the standard MASW processing routine. The phase-velocity estimation is preferable to the group-velocity estimation. For example, the dependence of the surface-wave wavenumber on the frequency commonly becomes linear at high frequencies: $k(f) = k_0 + \alpha f$. The group velocity becomes constant in this case: $u(f) = 1/\alpha$ — similar to the case in a homogeneous medium, but the phase velocity is not constant if k_0 is nonzero; thus, it can be inverted for a depth-dependent S-velocity profile.

Note, that the main method of dispersion imaging used in MASW is not the f-k method, but it is the phase-shift method by Park et al. (1998). Park et al. (1998) show that performing a spatial Fourier transform (FT) after a time FT is identical to applying a slant stack to the equivalent time-domain expression for a single frequency. In this sense, the f-k transform is similar to the phase-shift method in the f-k domain. Actually, the phase-shift method directly provides the phase-velocity frequency (v-f) image, which is usually used in surface-wave analysis, without interpolation (which in practice is necessary to obtain a v-f image from the f-k transform). However, we compare the proposed SFK method with the f-k transform because it also provides the image in the f-k domain.

METHOD

In practice, the surface-wave packet is often extracted by cutting out a corresponding part of the seismograms. This procedure is manually performed within a usual time-distance representation of the seismic recordings. A high-energy triangle area, which expands by the time and distance axes (because of the dispersion of the surface-wave velocities), is selected. This trick is the straightforward intuitive method to address the nonstationarity. A more advanced method is to consider the frequency-time representation of the seismic data.

Our proposed method consists of three steps. First, we obtain the frequency-time representation of the seismic data. Then, we analyze the obtained spectra in a slant-stacking manner but use a spatial FT instead of amplitude stacking. Finally, we build the resulting image by analyzing the f-k spectra for different steering values of surface-wave group velocities.

S-transform and surface waves

Kulesh et al. (2005) show how to estimate the group and phase velocities of dispersive waves using the continuous wavelet transform (CWT). Askari and Ferguson (2012) implement a similar method based on the S-transform, which provided a similar frequency-dependent resolution to the CWT. Unlike the CWT, the S-transform maintains a direct relationship with the Fourier spectrum (Stockwell et al., 1996). In particular, the S-transform properties make the estimation of surface-wave velocities more straightforward (Askari and Ferguson, 2012):

The S-transform of a signal $h(t)$ is given by

$$S[h(t)](\tau, f) = \int_{-\infty}^{+\infty} h(t) \frac{|f|}{\sqrt{2\pi}} e^{-\frac{(\tau-t)^2 f^2}{2}} e^{-i2\pi f t} dt. \quad (1)$$

As stated by Wu and Castagna (2017), for broadband seismic signals, such as a Ricker wavelet, the S-transform peak frequency is higher than the Fourier peak frequency. To solve this problem, Wu and Castagna (2017) introduce an unscaled S-transform by removing the normalization factor $|f|/\sqrt{2\pi}$ in equation 1. One can also introduce an additional wavelet-scaling parameter for resolution control (Pinnegar and Mansinha, 2003). However, here, we consider the classic S-transform 1, and the issues of improving the accuracy of the S-transform frequency-time representation in the proposed SFK method will be addressed in future research.

Let us observe a single mode of the surface wave. Consider two signals $h_1(t)$ and $h_2(t)$, which are recorded by two receivers of a linear acquisition system (both receivers are located on the same source-receiver line). The S-transform of the second signal can be expressed in terms of the S-transform of the first signal (for details, see Askari and Ferguson, 2012):

$$S[h_2(t)](\tau, f) = e^{-i2\pi k(f) l} e^{-\lambda(f) l} S[h_1(t)](\tau - k'(f) l, f), \quad (2)$$

where $k(f)$ is the wavenumber of the surface-wave, $\lambda(f)$ is a frequency-dependent attenuation parameter, and l is the distance between the two receivers. Askari and Ferguson (2012) use expression 2 to estimate the group $u(f) = 1/(k'(f))$ and phase $v(f) = f/k$ surface-wave velocities in the two-receiver framework, which is called the spectral analysis of surface waves. We propose a modification of S-transform wave propagation model 2 to emphasize the nonstationarity of the surface-wave packet with the MASW approach.

Consider a nonstationary surface-wave packet composed of a series of modes with wavenumbers $k_j(f)$, $j = 0,1, \ldots$. Let us apply the S-transform to each trace of a shot gather $g(x, t)$ and cut off the frequency axis at each frequency f. Thus, for each common frequency gather, we obtain a series of 2D complex-valued functions of the time and distance:

$$g_f(x, \tau) = S[g(x, t)](\tau, f, x), \quad (3)$$

which are called pseudoseismograms. The surface-wave packet traveltime curve for the time-distance coordinates of a common frequency pseudoseismogram is a slanted line. Assuming that a seismic source generates an impulse at zero time and offset, we introduce the S-transform nonstationary surface-wave packet model:

$$g_f^{\mathrm{surf}}(x, \tau) = \begin{cases} \sum_{k_j \in K[u,f]} A(u, f, x, k_j) e^{-2\pi i k_j x}, & \text{if } K[u, f] \neq \varnothing, \\ 0, & \text{if } K[u, f] = \varnothing, \end{cases} \quad (4)$$

where $u = x/\tau$ is a group-velocity, $A(u, f, x, k_j)$ is a real-valued amplitude factor, and $K[u, f] = \{k_j : k_j'(f) = u^{-1}\}$. Finally, we introduce the pseudoseismogram model:

$$g_f(x,\tau) = g_f^{\mathrm{surf}}(x,\tau) + \mu_f(x,\tau), \tag{5}$$

where $\mu_f(x,\tau)$ is an error term that contains the images of other seismic waves, noise, and modeling error. Signal model 5 underlies the SFK method. Signal model 5 is more appropriate for the description of the nonstationary surface wavefield than the common plane-wave model, underlying the standard spectral processing approaches. The problem is to estimate the wavenumbers $k_j(f)$, which are the parameters of the signal. Such kind of formulation — a parameter-estimation problem — is common in signal processing (Johnson and Dudgeon, 1992).

Slant-frequency-wavenumber analysis

For the fixed time frequency f and steering group velocity u, let us consider the 1D complex-valued function, which is defined by taking slant slices of the pseudoseismogram 3:

$$p_{uf}(x) = g_f\left(x, \frac{x}{u}\right), \tag{6}$$

which we call the slant-phase function. We suggest evaluating the phase function 6 for the group-velocity range $[u_{\min}, u_{\max}]$. The $u_{\min}$ is determined by a maximum moveout x_L and a maximum time T of the seismic records: $u_{\min} = x_L/T$; $u_{\max}$ is taken larger than the possible surface-wave velocity in the considered frequency range. We compute the slant-phase function 6 for a series of steering group-velocity values: $u_j = x_L/(T - jdt)$, where dt is the time-sampling rate. Note, that one should use interpolation to evaluate the slant-phase function 6 for the receiver positions $x_i < x_L$. In the next step, the amplitude of the slant-phase function FT is taken:

$$\Omega(u,f,k) = \left| \int_{-\infty}^{+\infty} p_{uf}(x) e^{-2\pi i x k} dx \right|. \tag{7}$$

Similar to the f-k transform, we use the fast FT to compute $\Omega(u,f,k)$. To achieve high resolution in the spectral region, we use zero padding (Foti et al., 2014). This is a standard operation and can be thought of as trace interpolation.

Thus, we obtain the spectral amplitude distribution in a 3D domain with the steering group velocity, frequency, and wavenumber as the coordinates. The spectral amplitude peaks of the slant-phase function correspond to the wavenumbers of plane waves, which travel directly from the source. All other waves are strongly suppressed, compared to the standard f-k processing.

Considering the amplitude dominance of the surface waves, for every pair (f,k), let us look for a maximum amplitude $\Omega(u,f,k)$ over all steering group velocities u:

$$P(f,k) = \max_u \Omega(u,f,k). \tag{8}$$

To select the surface-wave dispersion curves, we analyze the distribution 8 instead of the standard f-k and f-v images. The below flowchart, which is also presented in Figure 1, summarizes the SFK method:

$$(x,t) \xrightarrow{1} (f,x,\tau) \xrightarrow{2} (u,f,k) \xrightarrow{3} (f,k), \tag{9}$$

and represents the transfer from the (x,t) seismic gather domain to the (f,k) image domain. One can compare the SFK flowchart with the conventional f-k transform flowchart:

$$(x,t) \to (f,x) \to (f,k), \tag{10}$$

which assumes that the 2D FT is computed by two 1D FTs. The time localization of the surface-wave packet at each frequency during the SFK transform increases the signal-to-noise ratio (S/N) because of the exclusion of noise in other time steps (which does not fall in the effective width of the corresponding wavelet). The advantages of the SFK transform have been confirmed by synthetic- and field-data processing. Some of the results are presented in the next section of the paper.

In addition to f-k imaging, the SFK transform can be used to implement a joint analysis of the phase and group surface-wave velocities. For every point (f,k), the group-velocity steering values, which correspond to the maximum values that compose $P(f,k)$, can be taken:

$$U(f,k) = \arg\max_u \Omega(u,f,k). \tag{11}$$

Let us recall that to determine a phase-velocity dispersion curve from a group-velocity dispersion curve, it is sufficient if the phase velocity is only known at one point (Yanovskaya et al., 1988). A similar situation occurs on the (f,k) plane.

We interpret the distribution 11 as the group-velocity value of a hypothetical plane wave, whose phase-velocity dispersion curve passes through the point (f,k), and introduce the equation

$$\frac{df}{dk} = U(f,k). \tag{12}$$

The solutions of equation 12 are the phase lines (trajectories) of the following autonomous equation (Boyce and DiPrima, 2012):

$$\begin{aligned} \frac{dk}{ds} &= \frac{1}{\sqrt{U(f,k)^2+1}}, \\ \frac{df}{ds} &= \frac{U(f,k)}{\sqrt{U(f,k)^2+1}}. \end{aligned} \tag{13}$$

Starting from any point (f_0, k_0), one can trace (similar to the usual seismic ray-tracing manner) the phase trajectory $(f(s), k(s))$ using the obtained group-velocity distribution 11 by solving system 13 with the corresponding initial values: $k(s) = k_0$ and $f(s) = f_0$ at $s = 0$. Parameter s is a phase-trajectory length that starts from point (k_0, f_0) and moves in the direction of increasing frequency f.

One can check whether the dispersion curves, which are selected by analyzing the distribution $P(f,k)$ equation 8, coincide with the phase trajectories, which is defined by the equation 13. This

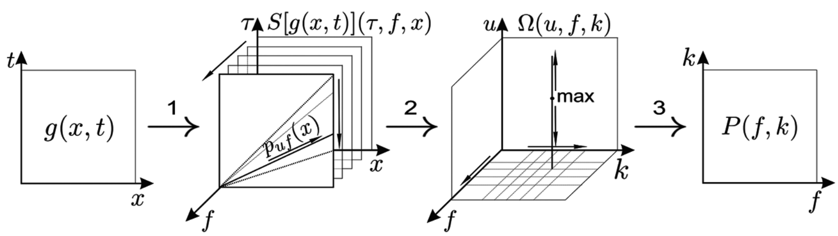

Figure 1. Schematic presentation of the SFK transform.

procedure can be used to control the reliability of the picked dispersion curves.

There are other possibilities to analyze the 3D spectral density 7. For example, it can be projected on the (u, f) plane by taking the maximum over the wavenumber k for fixed u and f. Thus, one can obtain an image to select the group-velocity dispersion curves. This approach appears similar to S-transform slant stacking, which was proposed by Askari and Hejazi (2015). However, analyzing the spatial spectrum appears more promising to decide whether there is a plane wave with the given group velocity in the data, than stacking the S-transform amplitudes.

EXAMPLES

To demonstrate the filtration properties of the proposed SFK method, let us present the spectral processing results of synthetic and field data sets. Because the SFK transform enhances f-k imaging technique, we compare the results with those obtained using the conventional 2D FT f-k transform. Similar to the conventional FT transform, we use standard receptions such as zero padding and accounting for spatial aliasing while transferring from f-k to the f-v domain (for details, see a book by Foti et al., 2014).

Table 1. Three-layered velocity model.

Layered seismic velocity model

Layer	V_S(m/s)	V_P(m/s)	ρ(g/cm^3)	Thickness(m)
1	300	500	1700	4
2	600	1500	1800	12
Half-space	1000	2000	2200	∞

Processing of data with random noise

Let us consider the three-layer stratified medium in Table 1. Using the matrix-propagator method, we computed the plane-wave synthetic seismic wavefield, which is only composed of a Rayleigh-wave fundamental mode. The source is described by a Ricker wavelet with a dominant frequency of 30 Hz. The resulting seismogram is shown in Figure 2a. The array consists of 20 receivers with 5 m spacing; a time-sampling rate of 2 ms is selected. We added Gaussian noise (S/N = −13.1 dB) to the data. The noisy data are presented in Figure 2b. It is impossible to visually observe a useful signal. However, the dispersion curve is clearly recognized in a wide range of frequencies in the f-k image, which was obtained by the proposed SFK method (see Figure 2c). The location of the spectral ridges and the calculated analytical dispersion curve, which is shown in black in Figure 2c, are consistent with each other. The dispersion curve is also observed in the conventional 2D FT f-k image, but it is strongly distorted (see Figure 2d). For this example, both images (Figure 2c and 2d) were normalized at each frequency (column-wise by dividing the entire vector by the maximum value).

Processing of field data

The receiver array consisted of 20 vertical 10 Hz geophones with 5 m spacing. The time-domain acquisition parameters were 1 s length and 2 ms sampling rate. A sledgehammer was used to generate a seismic impulse. The resulting seismogram is presented in Figure 3a. The f-k images are presented in Figure 3b (SFK) and 3c (2D FT). The normalized corresponding f-v images are shown in Figure 3c and 3d. In Figure 3b and 3d, one can observe well-defined images of three modes of surface waves. The 2D FT surface-wave images are notably strongly distorted (Figure 3c and 3e). The SFK spectral ridges are consistent with the phase trajectories; i.e., the curves $k = k(s)$, $f = f(s)$ on f-k plane that satisfy equation 13. Three trajectories, which pass through the corresponding local maximum of the f-k image, are plotted in black in Figure 3b and 3d. One can extend the surface-wave SFK phase trajectories to higher frequencies because the group velocities become constant. The multimode surface-wave dispersion curves can be used to improve the accuracy of the seismic S-wave velocity profiling (Lin and Ashlock, 2014). On the f-k image (see Figure 3c), it is clearly seen how the surface-wave energy dissipates at higher frequencies. Such a nonsmooth curve can hardly be interpreted within the framework of a stratified medium. We believe that it is caused by lateral heterogeneities.

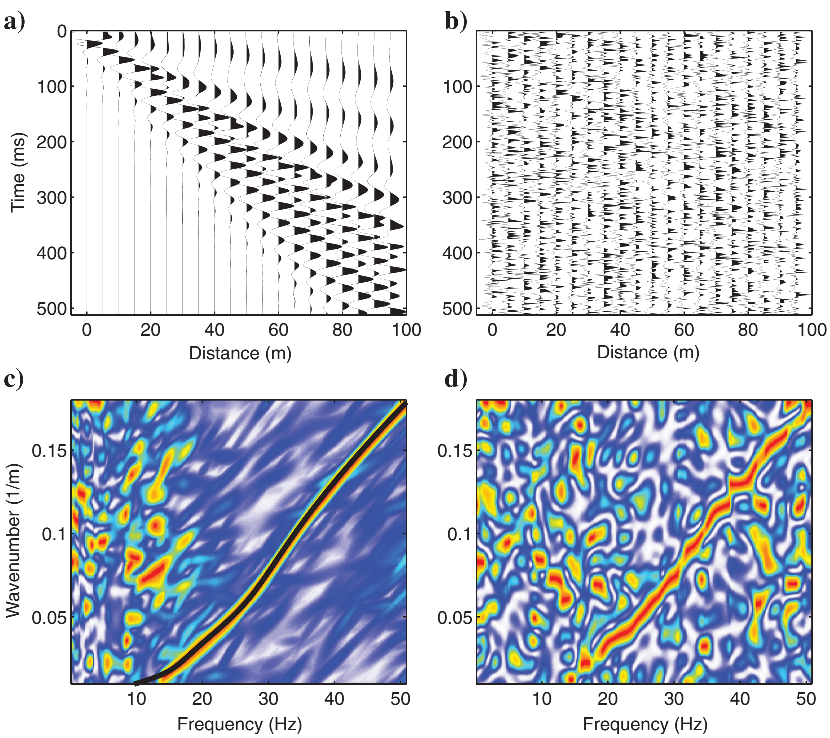

Figure 2. Synthetic data processing: (a) synthetic data without noise, (b) data with added Gaussian noise (S/N = −13.5 dB), (c) SFK-normalized f-k image of the data in (b), and (d) 2D FT-normalized f-k image of the data in (b).

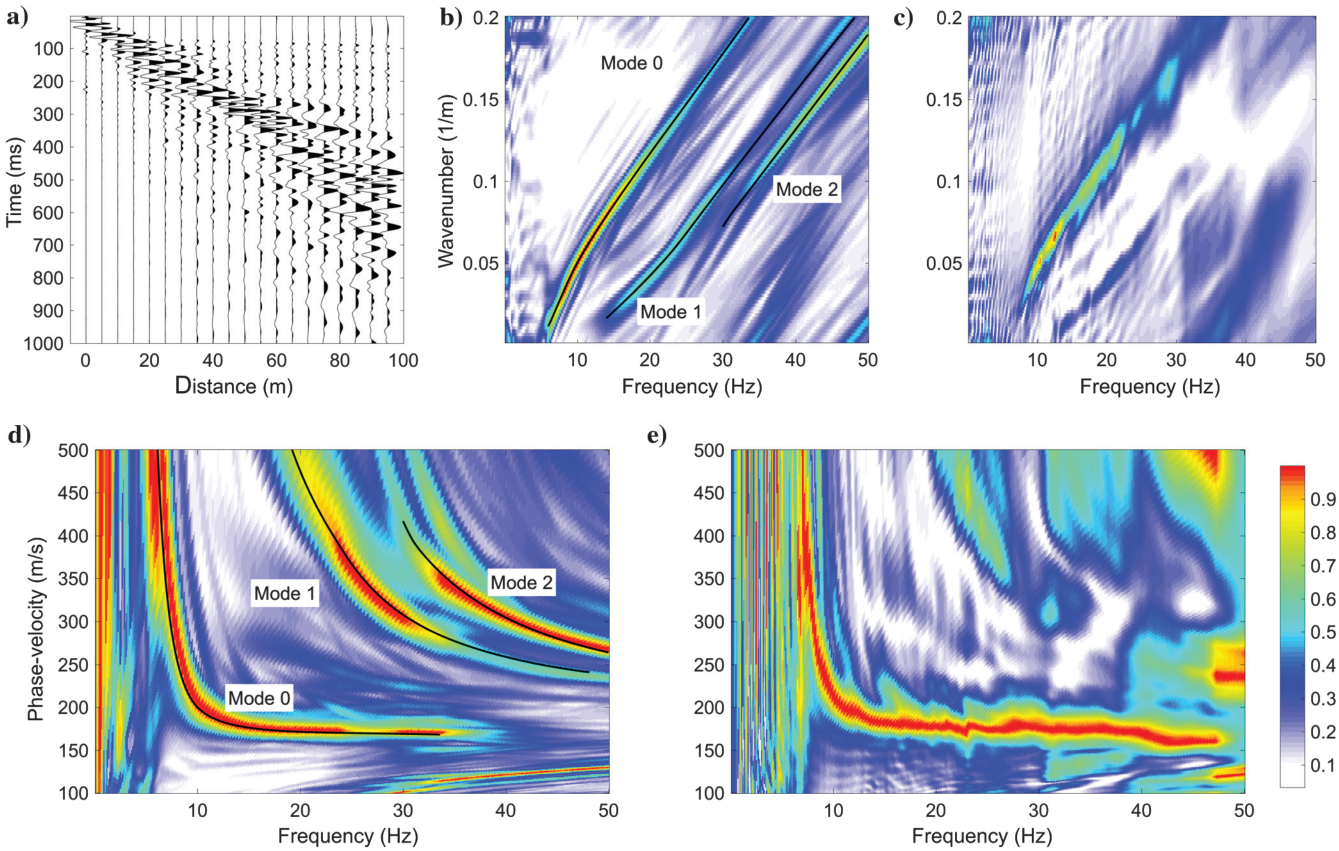

Figure 3. Field-data processing: (a) raw data, (b) SFK f-k image with three phase trajectories, corresponding to surface-wave dispersion curves (plotted in black), (c) 2D FT f-k image, (d) SFK f-v normalized image with three phase trajectories, corresponding to surface-wave dispersion curves (plotted in black), and (e) 2D FT f-v normalized image.

CONCLUSION

A new surface-wave multichannel data spectral processing method, which is called the slant frequency-wavenumber (f-k) transform, is proposed. We have tested the slant f-k transform on synthetic and field data, and we compared the results to the standard f-k results. Thanks to the use of the S-transform, i.e., a time-frequency representation, which preserves the phase spectrum, the wavenumber analysis is performed along the slanted lines. This approach excludes noise in the other time steps (which does not fall in the effective width of the corresponding wavelet) and reduces the spatial spectral leakage artifacts. Thus, the proposed slant f-k transform method is more robust than the standard f-k transform. The obtained results can be used in MASW to increase the accuracy of the estimation of shear velocities by inverting the surface-wave data.

ACKNOWLEDGMENTS

We are grateful for the comments by C. Park and two other anonymous reviewers that improved the manuscript. The research was supported by Russian Science Foundation (project no. 18-77-00043).

DATA AND MATERIALS AVAILABILITY

Data associated with this research are available and can be obtained by contacting the corresponding author.

REFERENCES

Askari, R., and R. J. Ferguson, 2012, Dispersion and the dissipative characteristics of surface waves in the generalized S-transform domain: Geophysics, **77**, no. 1, V11–V20, doi: 10.1190/geo2010-0330.1.

Askari, R., R. J. Ferguson, J. H. Isaac, and S. H. Hejazi, 2015, Estimation of S-wave static corrections using CMP cross-correlation of surface waves: Journal of Applied Geophysics, **121**, 42–53, doi: 10.1016/j.jappgeo.2015.07.004.

Askari, R., and S. H. Hejazi, 2015, Estimation of surface-wave group velocity using slant stack in the generalized S-transform domain: Geophysics, **80**, no. 4, EN83–EN92, doi: 10.1190/geo2014-0312.1.

Askari, R., and H. R. Siahkoohi, 2008, Ground roll attenuation using the S and x-f-k transforms: Geophysical Prospecting, **56**, 105–114.

Boyce, W. E., and DiPrima, 2012, Elementary differential equations and boundary value problems: Wiley.

Foti, S., C. G. Lai, G. J. Rix, and C. Strobbia, 2014, Surface wave methods for near-surface site characterization: CRC Press.

Johnson, D. H., and D. E. Dudgeon, 1992, Array signal processing: Concepts and techniques: Simon and Schuster.

Kulesh, M., M. Holschneider, M. S. Diallo, Q. Xie, and F. Scherbaum, 2005, Modeling of wave dispersion using continuous wavelet transforms: Pure and Applied Geophysics, **162**, 843–855, doi: 10.1007/s00024-004-2644-9.

Li, D., J. Castagna, and G. Goloshubin, 2016, Investigation of generalized S-transform analysis windows for time-frequency analysis of seismic reflection data investigation of GST analysis windows: Geophysics, **81**, no. 3, V235–V247, doi: 10.1190/geo2015-0551.1.

Lin, S., and J. C. Ashlock, 2014, Multimode Rayleigh wave profiling by hybrid surface and borehole methods: Geophysical Journal International, **197**, 1184–1195, doi: 10.1093/gji/ggu051.

Luo, Y., J. Xia, R. D. Miller, Y. Xu, J. Liu, and Q. Liu, 2008, Rayleigh-wave dispersive energy imaging using a high-resolution linear radon transform: Pure and Applied Geophysics, **165**, 903–922, doi: 10.1007/s00024-008-0338-4.

Mari, J., 1984, Estimation of static corrections for shear-wave profiling using the dispersion properties of love waves: Geophysics, **49**, 1169–1179, doi: 10.1190/1.1441746.
McMechan, G. A., and M. J. Yedlin, 1981, Analysis of dispersive waves by wavefield transformation: Geophysics, **46**, 869–874, doi: 10.1190/1.1441225.
Park, C. B., R. D. Miller, and J. Xia, 1998, Imaging dispersion curves of surface waves on multi-channel record: 68th Annual International Meeting, SEG, Expanded Abstracts, 1377–1380, doi: 10.1190/1.1820161.
Park, C. B., R. D. Miller, and J. Xia, 1999, Multichannel analysis of surface waves: Geophysics, **64**, 800–808, doi: 10.1190/1.1444590.
Pinnegar, C. R., and D. W. Eaton, 2003, Application of the S transform to prestack noise attenuation filtering: Journal of Geophysical Research: Solid Earth, **108**, doi: 10.1029/2002JB002258.
Pinnegar, C. R., and L. Mansinha, 2003, The S-transform with windows of arbitrary and varying shape: Geophysics, **68**, 381–385, doi: 10.1190/1.1543223.
Sacchi, M. D., and T. J. Ulrych, 1995, High-resolution velocity gathers and offset space reconstruction: Geophysics, **60**, 1169–1177, doi: 10.1190/1.1443845.
Shen, C., A. Wang, L. Wang, Z. Xu, and F. Cheng, 2015, Resolution equivalence of dispersion-imaging methods for noise-free high-frequency surface-wave data: Journal of Applied Geophysics, **122**, 167–171, doi: 10.1016/j.jappgeo.2015.09.019.
Socco, L. V., S. Foti, and D. Boiero, 2010, Surface-wave analysis for building near-surface velocity models: Established approaches and new perspectives: Geophysics, **75**, no. 5, 75A83–75A102, doi: 10.1190/1.3479491.
Stockwell, R. G., L. Mansinha, and R. Lowe, 1996, Localization of the complex spectrum: The S transform: IEEE Transactions on Signal Processing, **44**, 998–1001, doi: 10.1109/78.492555.
Tian, F., S.-M. Chen, E.-H. Zhang, J.-H. Gao, W.-C. Chen, Z.-Y. Zhang, and Y.-M. Li, 2002, Generalized S transform and its applications for analysis of seismic thin beds: 72nd Annual International Meeting, SEG, Expanded Abstracts, 2217–2220, doi: 10.1190/1.1817150.
Wu, L., and J. Castagna, 2017, S-transform and Fourier transform frequency spectra of broad-band seismic signals: Geophysics, **82**, no. 5, O71–O81, doi: 10.1190/geo2016-0679.1.
Xia, J., Y. Xu, and R. D. Miller, 2007, Generating an image of dispersive energy by frequency decomposition and slant stacking: Pure and Applied Geophysics, **164**, 941–956, doi: 10.1007/s00024-007-0204-9.
Yanovskaya, T., R. Maaz, P. Ditmar, and H. Neunhoefer, 1988, A method for joint interpretation of the phase and group surface-wave velocities to estimate lateral variations of the earth's structure: Physics of the Earth and Planetary Interiors, **51**, 59–67, doi: 10.1016/0031-9201(88)90023-4.
Yilmaz, Ö., 1987, Seismic data processing: SEG.